Low Temperature Physics/Fizika Nizkikh Temperatur, 2018, v. 44, No. 6, pp. 721–726

Entropy per particle spikes in the transition metal dichalcogenides

V.O. Shubnyi

Department of Physics, Taras Shevchenko National University of Kyiv
6 Academician Glushkov Ave., Kyiv 03680, Ukraine

V.P. Gusynin and S.G. Sharapov

Bogolyubov Institute for Theoretical Physics of the National Academy of Science of Ukraine
14-b Metrolohichna Str., Kyiv 03680, Ukraine
E-mail: vgusynin@bitp.kiev.ua

A.A. Varlamov

CNR-SPIN, University "Tor Vergata", Viale del Politecnico 1, I-00133 Rome, Italy

Received December 27, 2017, published online April 25, 2018

We derive a general expression for the entropy per particle as a function of chemical potential, temperature and gap magnitude for the single layer transition metal dichalcogenides. The electronic excitations in these materials can be approximately regarded as two species of the massive or gapped fermions. Inside the smaller gap there is a region with zero density of states where the dependence of the entropy per particle on the chemical potential exhibits a huge dip-and-peak structure. The edge of the larger gap is accompanied by the discontinuity of the density of states that results in the peak in the dependence of the entropy per particle on the chemical potential. The specificity of the transition metal dichalcogenides makes possible the observation of these features at rather high temperatures order of 100 K. The influence of the uniaxial strain on the entropy per particle is discussed.

PACS: 73.43.Cd Theory and modeling;
68.60.Dv Thermal stability; thermal effects;
65.40.gd Entropy.

Keywords: Dirac materials, entropy, dichalcogenides.

1. Introduction

We devote our work to the memory of Alexei Alexeyevich Abrikosov. One of the topics of his research at the end of the last millennium [1] was the unusual magnetoresistance, linear in magnetic field and positive, observed in nonstoichiometric silver chalcogenides. His approach was based on the assumption that these substances are gapless semiconductors with a linear energy spectrum discovered by himself with coauthors in sixties [2].

This work of Abrikosov had drawn attention of two authors of the present work (VG and SS) to the various realizations of the Dirac fermions in condensed matter systems. It was impossible to foresee that the discovery of graphene in 2004 would make the Dirac fermions in condensed matter one of the hottest topics of research for decades.

Another lesson that one may learn studying the scientific heritage of Alexei Abrikosov is to focus on the theoretical results that are closely related to experiment. He always taught that the article must be finished by the formula, which can be checked by experimentalist. Following his advice here we present a study of the entropy per particle $s = \partial S/\partial n$ (S is the entropy per unit volume and n is the electron density) for which a witty approach for experimental measurement was discovered by Kuntsevich *et al.* [3]. In spite of the fundamental character of entropy that characterizes thermodynamics, heat transfer, thermoelectric properties of many-body systems, it is always hard to measure it directly. The recent experiment [3] is not an exception as the quantity measured directly in a 2D electron gas is the temperature derivative of the chemical potential, $\partial\mu/\partial T$. The key idea of the authors of experiment [3] is that modu-

lation of the sample temperature changes the chemical potential and, hence, causes recharging of the gated structure, where the 2D electrons and the gate act as two plates of a capacitor. Therefore, $\partial\mu/\partial T$ is directly determined in the experiment from the measured recharging current. The Maxwell relation is then allows to equate both derivatives

$$s = \left(\frac{\partial S}{\partial n}\right)_T = -\left(\frac{\partial \mu}{\partial T}\right)_n . \quad (1)$$

It was theoretically predicted [4] that in a quasi-two-dimensional electron gas (2DEG) with parabolic dispersion, the entropy per electron exhibits quantized peaks when the chemical potential crosses the size quantized levels. The amplitude of such peaks in the absence of scattering depends only on the subband quantization number and is independent of material parameters, shape of the confining potential, electron effective mass, and temperature.

Very recently we studied [5] the behavior of s as a function of chemical potential, temperature and gap magnitude for the gapped Dirac materials. A special attention was paid to low-buckled Dirac materials [6,7], e.g., silicene [8] and germanene [9]. The dispersion law in these materials writes

$$\epsilon_{\eta s}(k) = \pm\sqrt{\hbar^2 v_F^2 k^2 + \Delta_{\eta\sigma}^2}, \quad (2)$$

where $\eta = \pm 1$ and $\sigma = \pm 1$ are the valley and spin indices, respectively. Here v_F is the Fermi velocity, k is the wavevector, and the valley- and spin-dependent gap, $\Delta_{\eta\sigma} = \Delta_z - \eta\sigma\Delta_{SO}$, where Δ_{SO} is the material dependent spin-orbit gap caused by a strong intrinsic spin-orbit interaction. It can have a relatively large value, e.g., $\Delta_{SO} \approx 4.2$ meV in silicene and $\Delta_{SO} \approx 11.8$ meV in germanene. The adjustable part of the gap $\Delta_z = E_z d$, where $2d$ is the separation between the two sublattices situated in different planes, can be tuned by applying an electric field E_z. Accordingly, the density of states (DOS) reads

$$D(\epsilon) = f(\epsilon)\sum_{i=1}^{N} \theta\left(\epsilon^2 - \Delta_i^2\right), \quad (3)$$

where the function $f(\epsilon)$ is assumed to be a continuous even function of energy ε and in the case of the discussed materials $N = 2$ and $f(\epsilon) = |\epsilon|/(\pi\hbar^2 v_F^2)$. The DOS (3) has 4 discontinuities at the points $\epsilon = \pm\Delta_i$, where $i = 1$ corresponds to $\eta = \sigma = \pm 1$ with $\Delta_1 = |\Delta_{SO} - \Delta_z|$ and the second one with $i = 2$ corresponds to $\eta = -\sigma = \pm 1$ with $\Delta_2 = |\Delta_z + \Delta_{SO}|$.

One of the main results predicted in [5] is that for $\mu = \pm\Delta_2$ ($\Delta_{SO}, \Delta_z > 0$ was assumed) there is a peak of the height $s = 2\ln 2/3$ in entropy per particle when $T \to 0$. The calculation of [5] shows that a peak at $\mu = \pm\Delta_2$ can still be seen for the temperature, $T \sim 10^{-2}\Delta_1$ for $\Delta_2 = 2\Delta_1$. Taking $\Delta_2 \sim \Delta_{SO}$, one estimates that the necessary temperature is the order of a few Kelvins.

Layered transition-metal dichalcogenides (TMDCs) represent another class of materials that can be shaped into monolayers, where similar effects might be observed. Single layer TMDCs with the composition MX_2 (where M = Mo, W is a transition metal, and X = S, Se, Te is a chalcogen atom) are truly two-dimensional (2D) semiconductors with a large band gap of the order of 1 eV to 2 eV (see, e.g., Refs. 10, 15). Consequently, one may expect that the peaks in entropy per particle can be seen at much higher temperatures.

The paper is organized as follows. We begin by presenting in Sec. 2 the model describing single layer TMDCs. Since the full description of strained TMDCs is very complicated, the effect of a uniform uniaxial strain is taken into account only via scalar potential spin-independent parts of the Hamiltonian. In Sec. 3 we discuss the DOS and present an analytical expression for the entropy per particle in TMDCs. The results for the obtained behavior of the entropy per particle are discussed in Sec. 4 and conclusions are given in Sec. 5.

2. Model

The low-energy excitations in monolayer TMDCs can be described by the following model Hamiltonian density [11–15]

$$H = \sum_{\tau=\pm 1} H_\tau, \qquad H_\tau = H_D^\tau + H_2, \quad (4)$$

where $\tau = \pm 1$ is the valley index, H_D^τ is the linear in momentum in Dirac-like part [16] and H_2 is the quadratic part. The Dirac Hamiltonian contains free massive Dirac fermion, H_0^τ, and spin-orbit term H_{SO}^τ, $H_D^\tau = H_0^\tau + H_{SO}^\tau$. The first term is

$$H_0^\tau = \hbar v_F(\tau k_x\sigma_x + k_y\sigma_y) + \frac{\Delta}{2}\sigma_z, \quad (5)$$

σ are the Pauli matrices acting in the 2×2 "band" space, σ_0 is the unit matrix, the Fermi velocity $v_F = at/\hbar \sim 0.5\cdot 10^6$ m/s with t being the effective hopping integral and a is the lattice constant, the major band gap $\Delta \sim 1$–2 eV. The inversion symmetry breaking results in the spin-orbit part of the Hamiltonian

$$H_{SO}^\tau = \lambda_v\tau\frac{\sigma_0 - \sigma_z}{2}s_z + \lambda_c\tau\frac{\sigma_0 + \sigma_z}{2}s_z, \quad (6)$$

where s_z is the Pauli matrix for spin, $2\lambda_v \sim 150$–500 meV is the spin splitting at the valence band top caused by the spin orbit coupling, $2\lambda_c$ is the spin splitting at the conduction band bottom. The DFT calculations [15] show that absolute value $2\lambda_v \gg |2\lambda_c| \sim 3$–$50$ meV and the sign of λ_c depends on the compound, $\lambda_c > 0$ for MoX_2 and $\lambda_c < 0$ for WX_2 compounds.

The quadratic part of the Hamiltonian, H_2, contains the following diagonal terms

$$H_2 = \frac{\hbar^2 k^2}{4m_e}(\alpha\sigma_0 + \beta\sigma_z), \tag{7}$$

where m_e is the free electron mass, and $\alpha \neq \beta$ are constants of the order of 1. Finally, as discussed in [11–15] more accurate approximations also include the trigonal warping terms.

The spin-up and spin-down components are completely decoupled, thus the spin index $\sigma = \pm 1$ is a good quantum number. Neglecting the quadratic term (7) we obtain the dispersion laws for conduction and valence bands

$$\epsilon_{c,v}(k) = \frac{\lambda_v + \lambda_c}{2}\tau\sigma \pm \sqrt{\hbar^2 v_F^2 k^2 + (\Delta - (\lambda_v - \lambda_c)\tau\sigma)^2/4}. \tag{8}$$

This spectrum closely resembles that of described by Eq. (2) of massive fermions in low-buckled Dirac materials except to the first valley- and spin-dependent term in Eq. (8). In the first approximation one can neglect the conduction band splitting and take $\lambda_c = 0$ to arrive at the simplest model [16], where the conduction bands remain spin degenerate at **K** and **K**′ points and have small spin splitting quadratic in **k**, whereas the valence bands are completely split,

$$\epsilon_{c,v}(k) = \frac{\lambda_v}{2}\tau\sigma \pm \sqrt{\hbar^2 v_F^2 k^2 + (\Delta - \lambda_v\tau\sigma)^2/4}. \tag{9}$$

Single layer TMDCs can sustain deformations higher than 10% [17,18]. The experimental possibility to tune the band gap with strain has been proven for MoS_2 in [19–22] and in WS_2 [23–25]. The full description of strained TMDCs is much more involved than that of graphene and includes five different fictitious gauge fields as well as scalar potentials entering spin-independent and spin-dependent parts of the Hamiltonian [26]. Below we restrict ourselves by a qualitative estimate of the strain effect on the properties of TMDCs and consider only the scalar potential term in the spin-independent Hamiltonian (5), viz.

$$H_{\rm str} = \frac{D_+(\hat{\varepsilon}) + D_-(\hat{\varepsilon})}{2}\sigma_0 + \frac{D_+(\hat{\varepsilon}) - D_-(\hat{\varepsilon})}{2}\sigma_3, \tag{10}$$

where $\hat{\varepsilon}$ is the strain tensor. The explicit expressions for the diagonal terms $D_\pm$ are provided in [26] and here we only keep the linear in strain contributions neglecting the higher order terms

$$D_\pm = \alpha_2^\pm(\varepsilon_{xx} + \varepsilon_{yy}), \tag{11}$$

with $\alpha_2^+ = -3.07$ eV and $\alpha_2^- = -1.36$ eV. The corresponding parameters for the spin-dependent part are smaller by the three orders of magnitude, so that the corresponding term can be safely neglected. Assuming that the strain is a uniform uniaxial one, we can express $D_\pm$ via $\varepsilon \equiv \varepsilon_{xx}$ ($\varepsilon > 0$ for tensile strain) and the Poisson's ratio, ν, [27] as follows $D_\pm = \alpha_2^\pm\varepsilon(1-\nu)$. Thus in the present toy model the effect of strain is reduced to renormalization of the chemical potential,

$$\mu \to \mu - \varepsilon(1-\nu)(\alpha_2^+ + \alpha_2^-)/2 \tag{12}$$

and the gap

$$\Delta \to \Delta + \varepsilon(1-\nu)(\alpha_2^+ - \alpha_2^-). \tag{13}$$

Setting $\nu = 0$ one may estimate that 1% tensile strain shifts μ by 22 meV and Δ by –17 meV, respectively.

3. Entropy per particle

As it was mentioned above, the entropy per particle is directly related to the temperature derivative of the chemical potential at the fixed density n (see Eq. (1)). The latter can be obtained using the thermodynamic identity

$$\left(\frac{\partial\mu}{\partial T}\right)_n = -\left(\frac{\partial n}{\partial T}\right)_\mu \left(\frac{\partial n}{\partial\mu}\right)_T^{-1}. \tag{14}$$

At thermal equilibrium, the total density of electrons is

$$n_{\rm tot}(T,\mu) = \int_{-\infty}^{\infty} d\epsilon D(\epsilon) f_{FD}\left(\frac{\epsilon - \mu}{T}\right), \tag{15}$$

where $f_{FD}(x) = 1/[\exp(x)+1]$ is the Fermi–Dirac distribution function and we set $k_B = 1$. Note that in the presence of the electron-hole symmetry it is convenient to operate with the difference n between the densities of electrons and holes instead of the total density of electrons, as usually done for graphene [5].

One can show that in a close analogy with graphene and low-buckled Dirac materials the DOS for TMDCs described by the approximate spectrum (8) is

$$D(\epsilon) = \frac{1}{\pi(\hbar v_F)^2}\sum_{i=\pm1}|\epsilon - \epsilon_i|\theta\left[(\epsilon-\epsilon_i)^2 - \Delta_i^2\right]. \tag{16}$$

Here we denoted $\epsilon_i = i(\lambda_v + \lambda_c)/2$ and $\Delta_i = [\Delta - i(\lambda_v - \lambda_c)]/2$ with $i = +1$ corresponding to $\tau = \sigma = \pm 1$ and $i = -1$ corresponding to $\tau = -\sigma = \pm 1$.

Obviously for $\lambda_c = 0$ the resulting DOS corresponds to the spectrum (9). The DOS (16) differs from the one described by the equation (3) by the presence of the energy shift, ϵ_i, in the modulus and in the argument of the θ-function. As a consequence the quantization of the entropy per particle, $s = \pm 2\ln 2/3$, obtained in [5] for the low-buckled Dirac materials does not occur in TMDCs.

The behavior of the DOS given by Eq. (16) is illustrated in Fig. 1. To be specific, we took the values $\Delta = 1.79$ eV, $2\lambda_v = 0.43$ eV corresponding to the compound WS_2. The constant $2\lambda_c$ for WS_2 is –0.03 eV [15]. In order to demonstrate the role of this parameter we choose the larger value of λ_c. Furthermore, we consider three possible cases: $\lambda_c = 0$ is shown by the dash-dotted (red) line, long dashed (green) line is for $\lambda_c = 0.05$ eV, dotted (blue) line is for

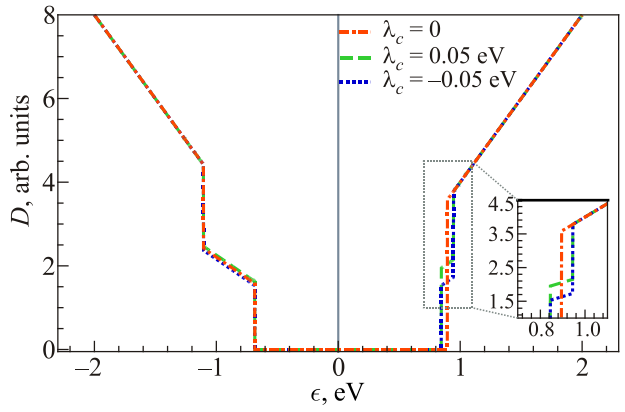

Fig. 1. (Colour online) The DOS, $D(\epsilon)$, in arbitrary units versus energy in eV. The parameters are $\Delta = 1.79$ eV, $2\lambda_v = 0.43$ eV. The dash-dotted (red) line $\lambda_c = 0$, long dashed (green) $\lambda_c = 0.05$ eV, dotted (blue) $\lambda_c = -0.05$ eV.

$\lambda_c = -0.05$ eV. Note that in general *ab initio* density functional theory calculations [15] predict that $\lambda_c > 0$ and $\lambda_c < 0$ correspond to MoX_2 and WX_2 compounds. Going from the negative to positive energies we observe the first discontinuity of the DOS at $\epsilon_{-1}^{-} = -\Delta/2 - \lambda_v = -1.11$ eV. It linearly goes down until the second discontinuity that occurs at $\epsilon_1^{-} = -\Delta/2 + \lambda_v = -0.68$ eV. Their positions are independent of the value of λ_c. The DOS is zero inside the gap between ϵ_1^{-} and $\epsilon_{-1}^{+} = \Delta/2 - \lambda_c$. Then it increases linearly until the discontinuity at the energy, $\epsilon_1^{+} = \Delta/2 + \lambda_c$. Obviously for $\lambda_c = 0$ the last two discontinuities become degenerate $\epsilon_{-1}^{+} = \epsilon_1^{+} = 0.895$ eV. For a finite λ_c their ordering depends on the sign of λ_c.

The peculiarities of DOS in TMDCs beyond the Dirac approximations are discussed in [28,29]. The quadratic part of the Hamiltonian (7) results in the curving of the linear in energy pieces seen in Fig. 1. Such curving is not essential and the does not change the discontinuous character of the DOS function that is responsible for the peaks in $s(\mu)$.

An advantage of the linearized approximation is that it resembles the case of gapped graphene and allows to obtain rather simple analytical results. For example, one can derive the analytical expression for the particle density (carrier imbalance) [30] and find the derivative $\partial\mu/\partial T$ using Eq. (14). Its generalization for the low-buckled Dirac materials was made in [5] (see also [31]). The expression for the particle density in TMDCs beyond the Dirac approximation is discussed in [29], but it is not very practical for obtaining the derivative $\partial\mu/\partial T$.

Differentiating Eq. (15) with respect to T and μ and shifting the variable of integration $\epsilon \to \epsilon + \epsilon_i$ for each term in the DOS (16) one obtains

$$\left(\frac{\partial n_{\rm tot}}{\partial T}\right)_{\mu} = \int\limits_{-\infty}^{\infty} \frac{d\epsilon(\epsilon-\mu)D(\epsilon)}{4T^2\cosh^2\dfrac{\epsilon-\mu}{2T}} = \sum_{i=\pm1} n_T(\mu_i,\Delta_i,T) \quad (17)$$

and

$$\left(\frac{\partial n_{\rm tot}}{\partial \mu}\right)_{T} = \int\limits_{-\infty}^{\infty} \frac{d\epsilon D(\epsilon)}{4T\cosh^2\dfrac{\epsilon-\mu}{2T}} = \sum_{i=\pm1} n_{\mu}(\mu_i,\Delta_i,T), \quad (18)$$

where $\mu_i = \mu - \epsilon_i$ is the shifted chemical potential. Since the corresponding integrands in Eqs. (17) and (18) become formally the same as in the case of the low-buckled Dirac materials [5] we arrive at the final expressions

$$n_T(\mu,\Delta,T) = \frac{1}{\pi\hbar^2 v_F^2}\left[\frac{\Delta}{T}\frac{\mu\sinh(\Delta/T)+\Delta\sinh(\mu/T)}{\cosh(\Delta/T)+\cosh(\mu/T)} + \right.$$
$$+ 2T\,{\rm Li}_2\left(-e^{-\frac{\mu+\Delta}{T}}\right) - 2T\,{\rm Li}_2\left(-e^{\frac{\mu-\Delta}{T}}\right) + \frac{2\Delta\mu}{T} -$$
$$\left. - (\mu-2\Delta)\ln\left(2\cosh\frac{\mu-\Delta}{2T}\right) - (\mu+2\Delta)\ln\left(2\cosh\frac{\mu+\Delta}{2T}\right)\right] \quad (19)$$

and

$$n_{\mu}(\mu,\Delta,T) = \frac{1}{\pi\hbar^2 v_F^2}\left[\frac{\Delta}{2}\left(\tanh\frac{\mu-\Delta}{2T} - \tanh\frac{\mu+\Delta}{2T}\right) + \right.$$
$$\left. + T\left(\ln\left(2\cosh\frac{\mu-\Delta}{2T}\right) + \ln\left(2\cosh\frac{\mu+\Delta}{2T}\right)\right)\right]. \quad (20)$$

${\rm Li}_2(x)$ in Eq. (19) is the dilogarithm function. As one can see, Eq. (20) is symmetric with respect to the transformation $\mu \to -\mu$ or $\Delta \to -\Delta$. On the other hand, Eq. (19) is antisymmetric under change $\mu \to -\mu$ and symmetric under $\Delta \to -\Delta$. The last property is checked using the identity for the dilogarithm function

$${\rm Li}_2\left(-\frac{1}{z}\right) = -{\rm Li}_2(-z) - \frac{1}{2}\ln^2(z) - \frac{\pi^2}{6}. \quad (21)$$

4. Results

Basing on obtained Eqs. (14), (19) and (20) one can investigate the dependence $s(\mu)$ for the different cases.

Figure 2 is computed for the material parameters Δ, λ_v and λ_c chosen for WS_2 compound. The dependence $s(\mu)$ is shown for three values of the temperature: the solid (red) line is for $T = 20$ K, the dashed (green) line is for $T = 40$ K and the dotted (blue) line is for $T = 80$ K. The vertical lines are at the values of chemical potential $\mu = \epsilon_{-1}^{-}, \epsilon_1^{-}, \epsilon_1^{+}, \epsilon_{-1}^{+}$ that correspond to the discontinuities of the DOS.

Comparing Fig. 2 with the results presented in [5], one can see that overall shape of $s(\mu)$ is similar for TMDCs and low-buckled Dirac materials, although the details are different. For example, inside the gap for $\mu \in [\epsilon_1^{-}, \epsilon_1^{+}]$ the dependence of s on the chemical potential exhibits a huge dip-and-peak structure in the temperature vicinity of the point $\mu = (\lambda_v + \lambda_c)/2$. (The value $i = 1$ corresponds to the smaller gap in Eq. (16).) This feature is even more pro-

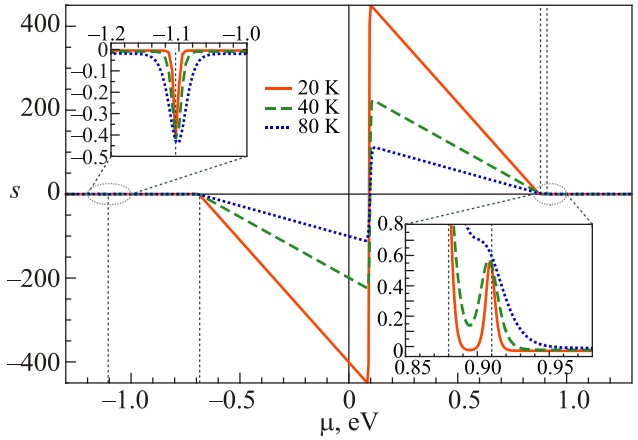

Fig. 2. (Colour online) The entropy per electron s vs the chemical potential μ in eV for three values of temperature. The parameters are $\Delta = 1.79$ eV, $2\lambda_v = 0.43$ eV and $\lambda_c = -0.015$ eV.

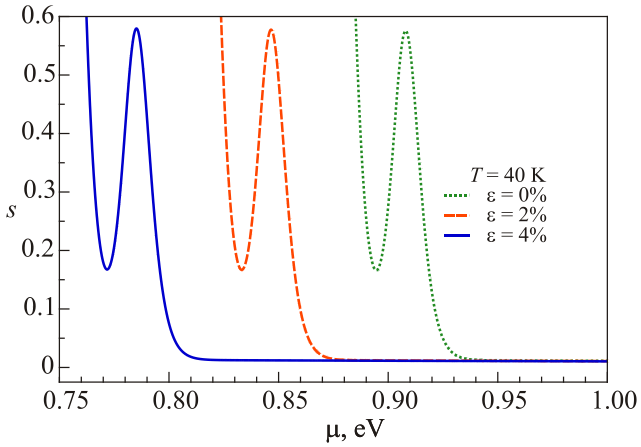

Fig. 4. (Colour online) The entropy per electron s vs the chemical potential μ in eV for three values of strain. The parameters are $\Delta = 1.79$ eV, $2\lambda_v = 0.43$ eV, $\lambda_c = -0.015$ eV, $\alpha_2^+ = -3.07$ eV, $\alpha_2^- = -1.36$ eV and $T = 40$ K.

nounced and sharp in TMDCs than in the other materials due to the larger ratio Δ/T. However in the low-buckled Dirac materials this structure was present in the temperature vicinity of the Dirac point, $\mu = 0$, because the whole dependence $s(\mu)$ was an antisymmetric function of μ. This is obviously not the case of TMDCs. As discussed in [5] the peak inside the gap is mainly due to the specific dependence of the chemical potential on the electron density.

The presence of the second larger gap, $\Delta_2 > \Delta_1$, in silicene and similar materials results in the emergence of the peak in $s(\mu)$ near the points $\mu = \pm\Delta_2$. Similarly the discontinuities of the DOS given by Eq. (16) at $\mu = \epsilon_{-1}^-, \epsilon_{-1}^+$ associated with a larger gap $i = 2$ also result in the peaks in $s(\mu)$. They are shown in the inserts in Fig. 2, because they are much smaller in height. As explained above the value of s at the peaks in the low-temperature limit is not equal to the quantized value $\pm 2\ln 2/3$ expected for the low-buckled Dirac materials [5]. It is essential that both peaks can still be seen at rather high temperatures. The peak on the right

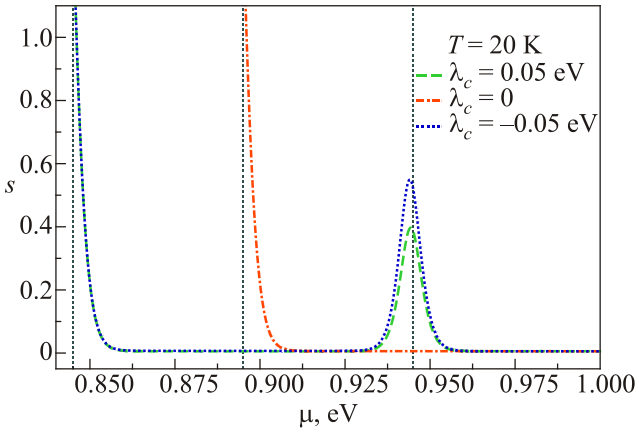

Fig. 3. (Colour online) The entropy per electron s vs the chemical potential μ in eV for three values of $\lambda_c = 0, \mp 0.05$ eV. The parameters are $\Delta = 1.79$ eV, $2\lambda_v = 0.43$ eV and $T = 20$ K.

starts to smear at $T = 80$ K, while the peak on the left can still be seen.

It is shown in Fig. 1 that for $\lambda_c = 0$ the two discontinuities of the DOS merge at $\mu = \epsilon_{-1}^+ = \epsilon_1^+$. Then the positive peak in $s(\mu)$ disappears as can be seen on the dash-dotted (red) in Fig. 3. As in Fig. 2 the vertical lines correspond to the singularities of the DOS. There is only one singularity for the dash-dotted (red) line at $\mu = \epsilon_{-1}^+ = \epsilon_1^+ = 0.895$ eV. For nonzero λ_c there are two singularities shifted from this point to the left and right by $|\lambda_c| = 0.05$ eV. In this case the peak at the larger energy $\mu = \Delta/2 + |\lambda_c|$ is restored as can be seen on the dotted (blue) line for $\lambda_c < 0$ and long dashed (green) line for $\lambda_c > 0$.

Finally we consider how a uniform uniaxial strain would affect the results shown in Fig. 2. We use Eqs. (12) and (13) to model the dependence of chemical potential and gap Δ on the strain, respectively. The dependence $s(\mu)$ is shown for three values of the strain: the dotted (green) line is for $\varepsilon = 0$, the dashed (red) line is for $\varepsilon = 2\%$ and the solid (blue) line is for $\varepsilon = 4\%$. As expected, the presence of strain results in the movement of the peaks in $s(\mu)$.

5. Conclusion

In the present work we had derived a general expression for the entropy per particle as a function of the chemical potential, temperature, and gap magnitude for the single layer transition metal dichalcogenides subjected to the uniform uniaxial strain. The spectrum of quasiparticle excitations of these materials is similar to that of the low-buckled Dirac materials, viz. there is the valley- and spin-dependent gap $\Delta_{\tau\sigma} = [\Delta - \tau\sigma(\lambda_v - \lambda_c)]/2$ in the spectrum. The difference from the latter is that the whole spectrum is also shifted by a valley- and spin-dependent constant $\epsilon_{\tau\sigma} = \tau\sigma(\lambda_v + \lambda_c)/2$. This introduces the hole-electron asymmetry in the band structure of TMDCs and makes the resulting DOS (16)

asymmetric function of the energy. When a small spin splitting at the conduction band bottom, λ_c, is taken into consideration the DOS (16) has 4 discontinuities: 2 for the negative and 2 for the positive energies. The positions of these discontinuities are not just at the energies $\pm|\Delta_{\tau\sigma}|$ with $\tau = \sigma = \pm 1$ and $\tau = -\sigma = \pm 1$ due to the energy shift $\epsilon_{\tau\sigma}$. It is demonstrated that inside the smaller gap there is a region with zero density of states where the dependence of the entropy per particle on the chemical potential exhibits a huge dip-and-peak structure. The edge of the larger gap is accompanied by the discontinuity of the density of states that results in the peak in the dependence of *s* on the chemical potential. The specifics of the transition metal dichalcogenides makes the found features to be of the "high temperature" nature, since they can be observed at rather high temperatures up to 100 K.

Since the Seebeck coefficient is related to the temperature derivative of the chemical potential, the strong peaks in the entropy per particle also indicate the same kind of singularities in the Seebeck coefficient in these materials. The latter can be expected at the edge of the gaps and has the origin similar to the electronic topological transitions [32–34].

Acknowledgment

We thank A.O. Slobodeniuk for illuminating discussion. We acknowledge the support of EC for the RISE Project CoExAN GA644076. V.P.G. and S.G.Sh. acknowledge a partial support from the Program of Fundamental Research of the Physics and Astronomy Division of the NAS of Ukraine No. 0117U00240.

1. A.A. Abrikosov, *Phys. Rev. B* **58**, 2788 (1998).
2. A.A. Abrikosov and S.D. Beneslavskii, *ZhETP* **59**, 1280 (1970) [*Sov. JETP* **32**, 699 (1971)].
3. A.Yu. Kuntsevich, I.V. Tupikov, V.M. Pudalov, and Y.S. Burmistrov, *Nat. Commun.* **6**, 7298 (2015).
4. A.A. Varlamov, A.V. Kavokin, and Y.M. Galperin, *Phys. Rev. B* **93**, 155404 (2016).
5. V.Yu. Tsaran, A.V. Kavokin, S.G. Sharapov, A.A. Varlamov, and V.P. Gusynin, *Sci. Rep.* **7**, 10271 (2017).
6. C.-C. Liu, W. Feng, and Y. Yao, *Phys. Rev. Lett.* **107**, 076802 (2011).
7. C.-C. Liu, H. Jiang, and Y. Yao, *Phys. Rev. B* **84**, 195430 (2011).
8. A. Kara, H. Enriquez, A.P. Seitsonen, L.C. Lew, Yan Voone, S. Vizzini, B. Aufray, and H. Oughaddou, *Surf. Sci. Rep.* **67**, 1 (2012).
9. A. Acun, L. Zhang, P. Bampoulis, M. Farmanbar, A. van Houselt, A.N. Rudenko, M. Lingenfelder, G. Brocks, B. Poelsema, M.I. Katsnelson, and H.J.W. Zandvliet, *J. Phys. Condens. Matter* **27**, 443002 (2015).
10. M. Chhowalla, H.S. Shin, G. Eda, L.-J. Li, K.P. Loh, and H. Zhang, *Nat. Chem.* **5**, 263 (2013).
11. E. Cappelluti, R. Roldán, J.A. Silva-Guillén, P. Ordejón, and F. Guinea, *Phys. Rev. B* **88**, 075409 (2013).
12. H. Rostami, A.G. Moghaddam, and R. Asgari, *Phys. Rev. B* **88**, 085440 (2013).
13. G.-B. Liu, W.-Y. Shan, Y. Yao, W. Yao, and D. Xiao, *Phys. Rev. B* **88**, 085433 (2013).
14. E. Ridolfi, D. Le, T.S. Rahman, E.R. Mucciolo, and C.H. Lewenkopf, *J. Phys.: Condens. Matter* **27**, 365501 (2015).
15. A. Kormányos, G. Burkard, M. Gmitra, J. Fabian, V. Zólyomi, N.D. Drummond, and V. Fal'ko, *2D Mater.* **2**, 049501 (2015).
16. Di Xiao, G.-B. Liu, W. Feng, X. Xu, and W. Yao, *Phys. Rev. Lett.* **108**, 196802 (2012).
17. S. Bertolazzi, J. Brivio, and A. Kis, *ACS Nano* **5**, 9703 (2011).
18. A. Castellanos-Gómez, M. Poot, G.A. Steele, H.S.J. van der Zant, N. Agrat, and G. Rubio-Bollinger, *Adv. Mater.* **24**, 772 (2012).
19. H.J. Conley, B. Wang, J.I. Ziegler, R.F. Haglund, S.T. Pantelides, and K.I. Bolotin, *Nano Lett.* **13**, 3626 (2013).
20. Y.Y. Hui, X. Liu, W. Jie, N.Y. Chan, J. Hao, Y.-T. Hsu, L.-J. Li, W. Guo, and S. P. Lau, *ACS Nano* **7**, 7126 (2013).
21. A. Castellanos-Gomez, R. Roldán, E. Cappelluti, M. Buscema, F. Guinea, H.S.J. van der Zant, and G. A. Steele, *Nano Lett.* **13**, 5361 (2013).
22. C.R. Zhu, G. Wang, B.L. Liu, X. Marie, X.F. Qiao, X. Zhang, X.X. Wu, H. Fan, P.H. Tan, T. Amand, and B. Urbaszek, *Phys. Rev. B* **88**, 121301 (2013).
23. Y. Wang, C. Cong, W. Yang, J. Shang, N. Peimyoo, Y. Chen, J. Kang, J. Wang, W. Huang, and T. Yu, *Nano Res.* **8**, 2562 (2015).
24. D. Voiry, H. Yamaguchi, J. Li, R. Silva, D.C. Alves, T. Fujita, M. Chen, T. Asefa, V.B. Shenoy, G. Eda, and M. Chhowalla, *Nat. Mater.* **12**, 850 (2013).
25. T. Georgiou, R. Jalil, B.D. Belle, L. Britnell, R.V. Gorbachev, S.V. Morozov, Y.-J. Kim, A. Gholinia, S.J. Haigh, O. Makarovsky, and L. Eaves, *Nat. Nanotechnol.* **8**, 100 (2013).
26. Gui-Bin Liu, Wen-Yu Shan, Yugui Yao, Wang Yao, and Di Xiao, *Phys. Rev. B* **88**, 085433 (2013).
27. L.D. Landau and E.M. Lifshitz, *Theory of Elasticity*, Pergamon Press, New York (1986).
28. A. Scholz, T. Stauber, and J. Schliemann, *Phys. Rev. B* **88**, 035135 (2013).
29. A. Iurov, G. Gumbs, D. Huang, and G. Balakrishnan, *Phys. Rev. B* **96**, 245403 (2017).
30. E.V. Gorbar, V.P. Gusynin, V.A. Miransky, and I.A. Shovkovy, *Phys. Rev. B* **66**, 045108 (2002).
31. A. Iurov, G. Gumbs, and D. Huang, *preprint arXiv: 1711.08485.*
32. A.A. Varlamov, V.S. Egorov, and A.V. Pantsulaya. *Adv. Phys.* **38**, 469 (1989).
33. Ya.M. Blanter, M.I Kaganov, A.V. Pantsulaya, and A.A. Varlamov, *Phys. Rep.* **245**, 159 (1994).
34. S.G. Sharapov and A.A. Varlamov, *Phys. Rev. B* **86**, 035430 (2012).